Mapping Heterogeneity in NanoTiO_2/ Polymer Coatings Using Confocal Microscopy and Depth Sensing Indentation

Li-Piin Sung, Yongyan Pang, Stephanie S. Watson, and Aaron M. Forster

Polymeric materials Group, Building and Fire Research Laboratory, National Institute of Standards and Technology, Gaithersburg, MD 20899

Introduction

The incorporation of nano-size fillers and structures into polymeric coatings and composites has the potential to provide advances in the performance of these materials compared to macro-/micrometer scale counterparts [1]. However, poor filler dispersion is qualitatively known to adversely affect the properties and ultimately the appearance, service life, and mechanical performance of polymeric systems. Traditional bulk testing methods, such as dynamic mechanical thermal analysis and tensile tests are not always suitable or sensitive to the physical or mechanical property changes in the local structural features upon addition of the nano-size fillers and structures, which are much smaller compared to the area of measurement. One of our major research objectives in the Polymeric Materials Group in the Building and Fire Research Laboratory is to develop relevant metrology to measure the appropriate structure-property relationship at a proper length scale to understand the interplay between nanoparticle and polymeric matrix.

In this paper, we present the preliminary results using a combination of laser scanning confocal microscopy (LSCM) and depth sensing indentation (DSI) techniques to probe and map surface/subsurface heterogeneity of the nanoparticle-filled polymeric coatings and to relate to their mechanical properties. Nanoparticle-polymer coating systems of different dispersion states were prepared using particle-polymer interactions in different polymer matrices. Two types of TiO_2 nanoparticles (with and without surface treatment) were chosen to mix into two different polymeric matrices. The heterogeneity in surface and subsurface was characterized using LSCM. The resultant surface mechanical properties were measured by DSI using different sizes and shapes of indenter tip. The best correlation was found for nanoparticle dispersion (cluster size and distribution) and surface modulus mapping while using a pyramidal shape tip.

Experimental[#]

Materials. Two commercially available nanoparticles were chosen for study: P25 TiO_2 (Evonik Degussa Corporation) (designated as P_A) and VHP-D TiO_2 (Altair) (P_B). The reported particle diameters for P_A and P_B from the manufacturer were about 25 nm and (30 – 40) nm, respectively. There is no surface treatment for P_A, but an organic solvent treatment was used for P_B. The measured particle/cluster size in a dilute particle water-borne paste suspension[*] for P_A is (127.4 ± 10.2) nm and P_B is (146.5 ± 5.6) nm determined by dynamic light scattering measurements (at NIST), implying that nanoTiO_2 particles form agglomerates in the suspensions.

Two polymeric matrices were used: two-component solvent-borne acrylic urethane (AU) and water-borne butyl-acrylic styrene latex (UCAR 481 from Dow Chemical) (Latex). Particle-filled coating films were prepared using a dispermat and a draw-down application on release paper. Detailed sample preparation, processing, and curing conditions were reported elsewhere [2-3]. Two particle volume concentrations (PVC) were studied, i.e. 2.5 %, and 5 %. Final thickness of dry films was ca. 110 μm for AU systems and ca. 80 μm for Latex systems.

Laser Scanning Confocal Microscopy (LSCM). A Zeiss model LSM510 reflection laser scanning confocal microscope (LSCM) was used with a laser wavelength of 543 nm to characterize the surface morphology and nanoTiO_2 spatial distribution on surface and near the surface. A detailed description of LSCM characterizations can be found elsewhere [4-5]. LSCM images are effectively the sum of all the light backscattered by different planar layers of the coating, as far into the film as light is able to penetrate and scatter back. Some of the LSCM images presented in this study are 2D projections, formed by summing the stack of images over the *z* direction (512 pixel x 512 pixel) of the coatings. The pixel intensity level represents the total amount of back-scattered light.

Depth Sensing Indentation (DSI). DSI measurements were performed using a NanoIndenter XP (Agilent Technologies). Two probe tip shapes were used, including a Berkovich pyramid, and a rounded cone with semi-apical angles of 45º and tip radius of 10 μm (tip angles and radii are nominal values provided by the manufacturer). The DSI experiments were conducted at a fixed strain rate of 0.05 s^{-1} and indented to a depth of 3 μm. This stiffness was used to calculate the elastic modulus of the sample [6-7] using a Poisson's ratio of 0.35, a representative value for polymers. Reported modulus values were average values obtained between the depths of 1000 nm - 2000 nm for 20 indents.

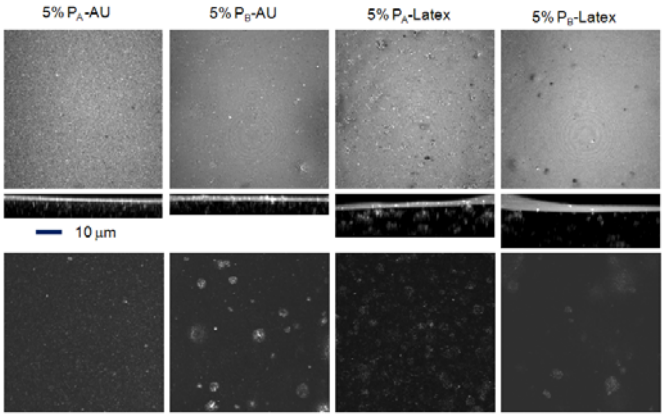

Figure 1. LSCM images of 2D projection (upper row), side projection (middle row), and a single-layer subsurface (bottom row) image for AU and Latex systems containing 5 % P_A and P_B. The scale bar is 10 μm.

Results and Discussion

Figure 1 displays the surface morphology of the coatings and the nanoTiO_2 distribution on the surface and subsurface. The surface appears to be rougher for both particles in the Latex system than in the AU system from the 2D projection images (upper row). The index of refraction of a TiO_2 particle is higher than that of the polymer matrix, and so the bright spots represent TiO_2 particles on or near the top surface, which scatter more light than the polymer binder. The 2D projection image of 5 % P_A-AU system shows smaller bright spots distributed uniformly in comparison to larger bright spots less uniformly distributed in the images of 5 % P_B-AU and 5 % P_A-Latex systems. There are very few bright spots on the surface of 5 % P_B-Latex. This implies most of TiO_2 particles were buried deep into the polymer binder. This observation is confirmed by the side projection images (middle row). For AU systems, the particles are distributed uniformly and tightly packed near the surface. The total scanning depth in the z direction (z-depth) is around 6 μm for both 5 % P_A-AU and 5 % P_B-AU system. Contrarily, for the latex systems, the particle clusters are loosely packed so that the z-depth is larger. For example, the total z-depth is about 17 μm for the 5 % P_B-Latex system.

This result is also reflected on the single-layer subsurface (depth profile) images in the bottom row (around 4 μm below the polymer-air surface). To further quantify the heterogeneity in these four systems in terms of nanoTiO_2 particle cluster size and distribution, a larger measured area with many LSCM depth profile images were analyzed

[#] Certain instruments or materials are identified in this paper in order to adequately specify experimental details. In no case does it imply endorsement by NIST or imply that it is necessarily the best product for the experimental procedure.

* The composition of the waterborne paste suspension is listed in the reference #2. Most composition are dispersant and surfactant in water.

using the NIH *ImageJ* program [8]. Figure 2 shows an example of the corresponding processed images with average cluster sizes obtained from a set of depth-profile LSCM images for AU and Latex systems containing 5 % of P_A and P_B. The result indicates (1) size of P_A clusters in both AU and Latex coatings is smaller than that of P_B clusters; (2) both P_A and P_B are distributed more uniformly in AU than in Latex; (3) 5 % P_A-AU system has a smaller cluster size and have the best particle dispersion; (4) the 5 % P_B-Latex system has the worst particle dispersion among the four systems.

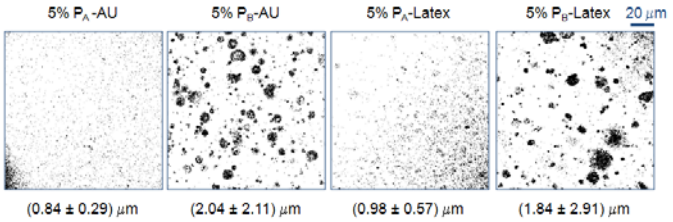

Figure 2. The processed images and the average cluster sizes obtained from a set of depth-profile LSCM images for AU and Latex systems containing 5 % of P_A and P_B. The scale bar is 20 μm. The ± values represent one standard deviation from the mean from 2000 particle counts.

Table 1. Surface modulus (E) of nanoTiO_2-AU coatings using DSI with two different tips. The E values of Pure AU are also listed as reference. The ± values represent one standard deviation from the average of 20 indents.

	Pure AU (GPa)	**5 % P_A-AU (GPa)**	**5 % P_B-AU (GPa)**
Pyramidal	3.62 ± 0.04	3.73 ± 0.04	4.12 ± 0.41
Cone	3.73 ± 0.04	3.98 ± 0.03	4.29 ± 0.36

The effect of heterogeneity in the surface and subsurface of the coatings on the surface mechanical properties was investigated using DSI technique with different tip shapes. As mentioned previously, the 5 %P_A-AU system has a smaller cluster size and better distribution than the 5 % P_B-AU system. Some P_B clusters in AU are as large as 10 μm (see Figure 2) and a higher variation is expected in the surface mechanical measurements due to the heterogeneity of larger cluster distribution. Table 1 summarizes the surface modulus (E) data for AU systems obtained from two different tips: Berkovich pyramid and 10 μm cone tips. With an addition of 5 % P_B, the E values increase noticeably from pure AU but with a larger deviation using both tips. However, this result do not clearly reflect and correlate with the heterogeneity on the surface or subsurface of P_B-AU system.

Note that the E values were evaluated between the probing depths between 1000 nm and 2000 nm. So that it is important to examine the E values as a function of location and depth into the surface. Figures 3a-b show the 9 residual indented marks for 5 % P_A-AU and 5 % P_B-AU systems using a pyramidal shape tip and their modulus-displacement (m-d) curves for four selected marks. There is no difference observed in the m-d curves for all intended marks in the 5 % P_A-AU system (same results were found using the cone tip). All residual indented marks look the same and remain a symmetrical pyramidal shape (Figure 3a). On the other hand, there are a few of residual indented marks with irregular shape, such as marks #1, #2 and #4 in Figure 3b for 5 % P_B-AU systems using a pyramidal shape tip. These extended or distorted corners of the pyramidal shape are correlated to location of the P_B clusters on or near the surface (see subsurface images - Figure 3b middle graph). Moreover, it is consistent with the distribution of clusters in the depth profile and the m-d cure shown in the bottom graph of Figure 3b. For example, for a P_B cluster on the surface (mark #4), a higher E value was observed immediately into the surface. While for mark #1 (or mark #2), the E values increase gradually until the indenter encounters the effect of a P_B cluster in the subsurface. Figure 3c also shows the residual indented marks with the corresponding subsurface image, and the selected m-d curves for the 5 % P_B-AU system using a cone tip. The changes observed in this case are not as noticeable as in Figure 3b using a pyramidal shape tip. Further investigation to establish the correlation between surface modulus mapping (using the m-d curves) and the nanoTiO_2 cluster distribution in various coating systems is ongoing.

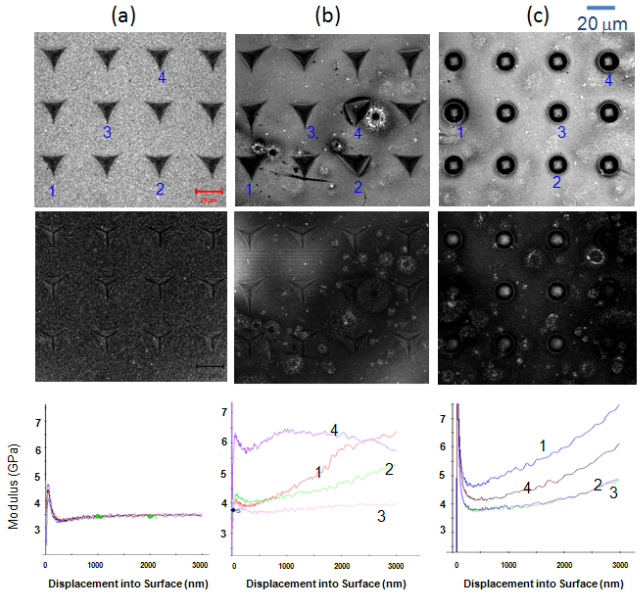

Figure 3. Residual indented marks on (a) 5 % P_A-AU system (b) 5 % P_B-AU system using a pyramidal shape tip, and (c) 5 % P_B-AU system using a Cone shape tip. The middle graphs show a single-layer subsurface image ca 3 μm below the polymer-air surface. Scale is 20 μm. The lower graphs show surface modulus as a function of displacement into surface for four indented masks as indicated in the upper graphs.

Summary

A combination of laser scanning confocal microscopy and depth sensing indentation techniques provides a powerful tool to probe and map surface/subsurface heterogeneity of the nanoparticle-filled polymeric coatings and to relate to their surface mechanical properties.

References

1. *ACS Symposium Series1008:* Nanotechnology Applications in Coatings, Eds.: Fernando, R.H.; Sung, L., ACS/Oxford University Press, Washington DC, June **2009**.
2. Pang, Y.; Sung, L.; Watson, S.S., ACS Polymeric Materials: Science & Engineering, 101, 1516, **2009**.
3. Flick, E.; *Water-Based Paint Formulation* 4, Noyes Publication, Westwood, NJ, 1994, p34.
4. Sung, L.; Jasmin, J.; Gu, X.; Nguyen, T.; and Martin, J.W. *JCT Research* **2004**, 1, 267.
5. Faucheu, J.; Sung, L.P.; Martin, J.W.; Wood, K.A., *J. Coat. Technol. Res.,* **2006**, 3 (1), 29-39.
6. VanLandingham, M.R. *Journal of Research of the National Institute of Standards and Technology* **2003**; 108, 249.
7. Sung, L. ; Comer, J. ; Forster, A.M.; Hu, H.; Floryancic, B. ; Brickweg,L. ; Fernando, R.H. ; *J. Coat. Technol. and Res*., **2008**, 5(4) 419**.**
8. The NIH freeware *ImageJ* program can be downloaded from http://rsbweb.nih.gov/ij/download.html.